Self-screening of the quantum confined Stark effect by the polarization induced bulk charges in the quantum barriers

Zi-Hui Zhang, Wei Liu, Zhengang Ju, Swee Tiam Tan, Yun Ji, Zabu Kyaw, Xueliang Zhang, Liancheng Wang, Xiao Wei Sun, and Hilmi Volkan Demir

Articles you may be interested in

Influence of quantum-confined Stark effect on optical properties within trench defects in InGaN quantum wells with different indium content
J. Appl. Phys. **115**, 213512 (2014); 10.1063/1.4881776

Quantum-confined stark effect in localized luminescent centers within InGaN/GaN quantum-well based light emitting diodes
Appl. Phys. Lett. **101**, 121919 (2012); 10.1063/1.4754079

Quantum-confined Stark effects in the m -plane In 0.15 Ga 0.85 N Ga N multiple quantum well blue light-emitting diode fabricated on low defect density freestanding GaN substrate
Appl. Phys. Lett. **91**, 181903 (2007); 10.1063/1.2802042

Electroreflectance studies of Stark shifts and polarization-induced electric fields in InGaN/GaN single quantum wells
J. Appl. Phys. **95**, 4905 (2004); 10.1063/1.1690100

Band alignment and barrier height considerations for the quantum-confined Stark effect
J. Vac. Sci. Technol. A **16**, 801 (1998); 10.1116/1.581061

Self-screening of the quantum confined Stark effect by the polarization induced bulk charges in the quantum barriers

Zi-Hui Zhang,[1] Wei Liu,[1] Zhengang Ju,[1] Swee Tiam Tan,[1] Yun Ji,[1] Zabu Kyaw,[1] Xueliang Zhang,[1] Liancheng Wang,[1] Xiao Wei Sun,[1,a)] and Hilmi Volkan Demir[1,2,a)]

[1]*LUMINOUS! Centre of Excellence for Semiconductor Lighting and Displays, School of Electrical and Electronic Engineering, School of Physical and Mathematical Sciences, Nanyang Technological University, 50 Nanyang Avenue, Singapore 639798*
[2]*Department of Electrical and Electronics, Department of Physics, and UNAM-Institute of Material Science and Nanotechnology, Bilkent University, TR-06800 Ankara, Turkey*

InGaN/GaN light-emitting diodes (LEDs) grown along the polar orientations significantly suffer from the quantum confined Stark effect (QCSE) caused by the strong polarization induced electric field in the quantum wells, which is a fundamental problem intrinsic to the III-nitrides. Here, we show that the QCSE is self-screened by the polarization induced bulk charges enabled by designing quantum barriers. The InN composition of the InGaN quantum barrier graded along the growth orientation opportunely generates the polarization induced bulk charges in the quantum barrier, which well compensate the polarization induced interface charges, thus avoiding the electric field in the quantum wells. Consequently, the optical output power and the external quantum efficiency are substantially improved for the LEDs. The ability to self-screen the QCSE using polarization induced bulk charges opens up new possibilities for device engineering of III-nitrides not only in LEDs but also in other optoelectronic devices. © 2014 AIP Publishing LLC. [http://dx.doi.org/10.1063/1.4883894]

In the past several decades, InGaN/GaN light-emitting diodes (LEDs) have gained tremendous development in the epitaxial growth, chip fabrication, and the optoelectronic device physics.[1,2] Even so, there are still quite a few formidable challenges limiting the LED performance. On one hand, the crystal quality of the epitaxial LED wafers has room to be further improved,[3] which will help to suppress the carrier loss through the defect-related nonradiative recombination.[4,5] On the other hand, the Auger recombination is rendered as another carrier loss channel in the multiple quantum well (MQW) region.[6,7] Moreover, the InGaN/GaN LEDs grown along [0001] orientation suffer from the strong polarization induced electric fields, and the resulted tilted energy band leads to a spatial separation of the carrier wave functions and thus a reduced radiative recombination rate, known as the quantum confined Stark effect (QCSE). One way to reduce the QCSE is to suppress the polarization by growing the InGaN/GaN LEDs along those nonpolar or semipolar orientations.[8–11] Even in LEDs grown along [0001] orientation, the polarization in the InGaN/GaN MQWs can be suppressed by embedding the InGaN quantum well between the polarization matched quaternary AlInGaN quantum barriers.[12] Apart from the above methods, the polarization induced electric field within the quantum wells can be screened by Si doping the quantum barriers.[13] According to the report by Zhang *et al.*,[13] in addition to the electrons released by those Si dopants in the quantum barriers, the ionized Si dopants are also essential in screening the polarization induced electric field within the quantum wells, and thus the QCSE. The drawback of a high Si doping level in the

quantum barriers is that it will block the hole injection across the whole active region.[13] Therefore, it will be useful to replace those ionized dopants with any other electrically charged particles which can avoid the hole blocking effect. Hence, in this work, we have proposed the $In_yGa_{1-y}N/In_xGa_{1-x}N$ quantum well/quantum barrier architecture, in which the InN composition x in the quantum barrier is graded along the growth direction, so that the polarization induced bulk charges are generated to replace the ionized dopants in the quantum barriers, and have an excellent screening effect on the polarization induced electric field in the quantum wells.

The physics of the generation of the polarization induced bulk charge in the $In_yGa_{1-y}N/In_xGa_{1-x}N$ quantum well/quantum barrier architecture is explained first as follows. As known, the $In_yGa_{1-y}N/In_xGa_{1-x}N$ heterostructures grown along the polar orientations are not geometrically symmetric, such that the geometrical centres of those more/less ionic atoms in the lattice are not coincident. Therefore, the polarization charges are generated at the $In_yGa_{1-y}N/In_xGa_{1-x}N$ interface. For a two-dimensional (2D) charge profile, the interface charge density is represented by $\sigma_S^{pol} = n \cdot P$, where P represents the polarization density and n denotes the unit vector normal to the $In_yGa_{1-y}N/In_xGa_{1-x}N$ interface. However, the above equation is invalid once the charge profile is not confined within the 2D surface. Then the polarization induced charge density has to be calculated by $\rho_B^{Pol}(z) = \nabla \cdot P(z)$,[14] where the $P(z)$ denotes the polarization density in terms of the grading position (z). The aforementioned equation can be further modified to $\rho_B^{Pol}(z) = \nabla \cdot P(z) = (\partial P/\partial x) \times (\partial x/\partial z)$ by considering the polarization density as a function of the InN composition (i.e., x) in the $In_yGa_{1-y}N/In_xGa_{1-x}N$ heterojunction. We

a)Authors to whom correspondence should be addressed. Electronic addresses: exwsun@ntu.edu.sg and volkan@stanfordalumni.org
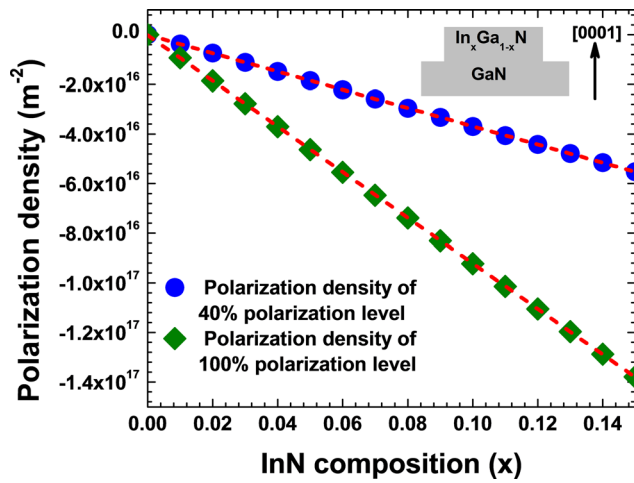
© 2014 AIP Publishing LLC

FIG. 1. Polarization density in terms of the InN composition for the $In_xGa_{1-x}N$ layer grown on the GaN template. Both 40% and 100% polarization levels are assumed.
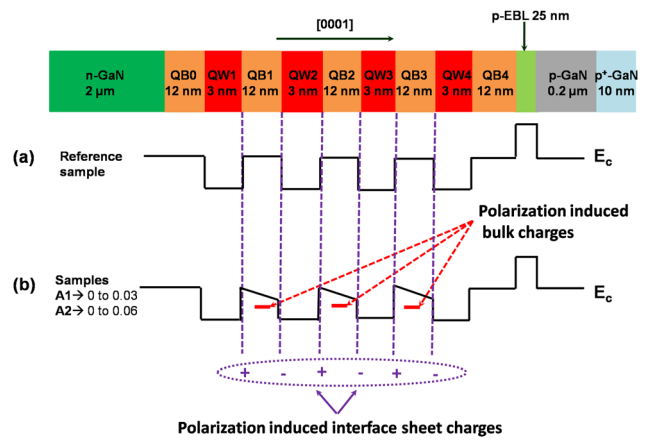

FIG. 2. Schematic conduction band diagrams for the studied samples: (a) reference sample; (b) Samples A1 and A2, along with which also show the distribution of the polarization induced sheet charges and the polarization induced bulk charges. E_c denotes the conduction band.

have shown the polarization density in terms of the InN composition in Fig. 1. The calculation is based on the model developed by Fiorentini *et al.*[15] In Fig. 1, we have shown the relationship between P and x for the 40% and 100% polarization levels, respectively. The polarization level means how many percentiles of the theoretical predicted polarization charges are included by considering the crystal relaxation through the dislocation generations.[15] Clearly, we can see from Fig. 1 that the polarization density of the 100% polarization level is larger than that of the 40% polarization level. However, both curves have shown a linear relationship as the InN composition varies. Therefore, $\partial P/\partial x$ is $-3.68 \times 10^{17}\,m^{-2}$ and $-9.19 \times 10^{17}\,m^{-2}$ for the 40% and 100% polarization levels, respectively. Moreover, the $\rho_B^{Pol}(z)$ is also influenced by $\partial x/\partial z$, which is also a constant once the InN composition (x) is linearly graded along the growth orientation. Thus, $\rho_B^{Pol}(z)$ is treated as the bulk charge density, and thus, $\left[\rho_B^{Pol}(z)\right] = m^{-3}$. These polarization induced bulk charges will have a positive effect on the screening of QCSE and the performance improvement of the LEDs.

To investigate the screening effect of the QCSE by the polarization induced bulk charges in the quantum barriers, several $In_yGa_{1-y}N/In_xGa_{1-x}N$ LED samples [Figs. 2(a) and 2(b)] have been grown by the metal-organic chemical vapour deposition (MOCVD) system. The c-plane sapphires are used as the substrates for the LED samples. The growth was initiated from a 20 nm thick GaN nucleation layer and followed by a $4\,\mu m$ thick unintentionally doped n-type GaN (u-GaN) layer. A $2\,\mu m$ n-type GaN layer with Si doping concentration of $5 \times 10^{18}\,cm^{-3}$ serves as the electron injection layer, and the diluted SiH_4 is used as the precursor for the Si dopants. Then four-period MQWs were grown for all

samples, in which the quantum well and quantum barrier thickness are 3 nm and 12 nm, respectively. The InN composition in the quantum wells is 15%. The samples differ only in their quantum barriers. The reference sample has employed the GaN as the quantum barriers. However, for other LED samples, the $In_xGa_{1-x}N$ is used as their quantum barriers. In Samples A1 and A2, the InN composition has been linearly increased from 0 to 0.03 and 0 to 0.06 along the [0001] growth orientation, respectively. However, the other quantum barriers (i.e., QB0 and QB4) for all samples were the 12 nm thick GaN layers. On top of the MQWs, a 25 nm thick p-type $Al_{0.20}Ga_{0.80}N$ electron blocking layer (EBL) was grown and followed by a $0.2\,\mu m$ p-GaN hole injection layer. Mg is utilized as the p-type dopants for the p-type electron blocking layer and the p-GaN layer, in which the effective hole concentration is estimated to be $3 \times 10^{17}\,cm^{-3}$. Finally, a heavily doped p$^+$-GaN layer of 10 nm was grown serving as the ohmic contact layer.

In addition, Figs. 2(a) and 2(b) have also demonstrated the charge profiles for all the samples. The details of the polarization induced sheet charge density (σ_S^{Pol}) and the polarization induced bulk charge density (ρ_B^{Pol}) are illustrated in Table I. The calculation has assumed the 40% polarization level by taking the crystal relaxation into consideration.[15]

The electroluminescence (EL) and the optical output power for all the samples have been collected through an integrating sphere attached to an Ocean Optics spectrometer (QE65000). The metal contacts were made by indium on the LED wafers with a diameter of 1.0 mm.

The measured peak emission wavelengths in terms of the injection current level for the reference sample, Samples A1 and A2 have been demonstrated in Fig. 3. We can see

TABLE I. Calculated σ_S^{Pol} at the quantum well/quantum barrier interface and ρ_B^{Pol} in the $In_xGa_{1-x}N$ quantum barriers with different InN composition grading configurations.

	$In_{0.15}Ga_{0.85}N/GaN$	$In_{0.15}Ga_{0.85}N/In_{0.03}Ga_{0.97}N$	$In_{0.15}Ga_{0.85}N/In_{0.06}Ga_{0.94}N$
σ_S^{Pol}	$0.55 \times 10^{17}\,m^{-2}$	$0.44 \times 10^{17}\,m^{-2}$	$0.33 \times 10^{17}\,m^{-2}$
ρ_B^{Pol}	$In_{0.03}Ga_{0.97}N \leftarrow \rightarrow GaN$ within 12 nm		$In_{0.06}Ga_{0.94}N \leftarrow \rightarrow GaN$ within 12 nm
	$9.19 \times 10^{23}\,m^{-3}$		$1.84 \times 10^{24}\,m^{-3}$

that the initial peak wavelength at 5 A/cm² for the reference sample is ∼460 nm. However, the peak emission wavelength has been reduced to ∼446 nm for Sample A1 and ∼437 nm for Sample A2, respectively. Since the growth conditions (e.g., growth pressure and growth temperature) of the quantum well regions for the studied samples are identical, the InN composition variation in the quantum well is less likely to cause the large wavelength blue shift.[16] Thus, the blue shift of the emission wavelength for Samples A1 and A2 compared to the reference sample is well attributed to the suppressed polarization induced electric field within the quantum well[13] by the InN composition grading in the quantum barriers. Moreover, because of the strongest polarization induced electric field in the quantum wells for the reference sample, the emission wavelength has been shifted by ∼0.89% ($\Delta\lambda = \sim4.1$ nm) when the current increases to 20 A/cm² from 5 A/cm². As the polarization induced electric field in the quantum wells for Sample A1 has been relieved, the wavelength is shifted by ∼0.7% ($\Delta\lambda = \sim3.0$ nm) in the same current density range. An even smaller wavelength shift of ∼0.5% ($\Delta\lambda = \sim2.0$ nm) for Sample A2 is observed in the same current density range; thanks to the further screening of the polarization induced electric field in the quantum wells.

As reported, the polarization induced electric field in each layer of a periodic heterostructure stack such as the InGaN/GaN MQWs can be mathematically expressed by the following equation:[17]

$$E_j = \frac{\sum_{k=1}^{n} l_k \cdot P_k / \varepsilon_k - P_j \cdot \sum_{k=1}^{n} l_k / \varepsilon_k}{\varepsilon_j \cdot \sum_{k=1}^{n} l_k / \varepsilon_k}, \tag{1}$$

where E_j is the electric field in the jth layer, l_k, and ε_k are the thickness and dielectric constant for each layer while P_k is the polarization density in the kth layer. However, if we assume the electric field in the quantum well/quantum barrier is mainly affected by its adjacent quantum barriers/quantum wells, Eq. (1) can be further simplified to the following set of equations:

$$E_w \approx \frac{l_b \cdot \Delta P}{l_b \cdot \varepsilon_w + l_w \cdot \varepsilon_b}, \tag{2a}$$

$$E_b \approx \frac{l_w \cdot \Delta P}{l_b \cdot \varepsilon_w + l_w \cdot \varepsilon_b}. \tag{2b}$$

Thus, $E_b \cdot l_b = E_w \cdot l_w$ where E_b and E_w are the electric fields in the quantum barrier and quantum well, respectively. Note that the direction of the electric field in the quantum barrier is opposite to that in the quantum well. The dielectric constants for the quantum barrier and the quantum well are represented by ε_b and ε_w, respectively. The thickness of the quantum barrier and the quantum well is l_b and l_w, respectively. ΔP represents the net polarization charge density. Therefore, one way to reduce the polarization induced electric field within the quantum well (i.e., E_w) is to reduce $E_b \cdot l_b$. One can either reduce the quantum barrier thickness of l_b or the polarization induced field of E_b in the quantum barriers. In this work, we have achieved a reduced E_w by reducing the E_b. According to Eq. (2b), the E_b can be reduced through decreasing the net polarization charge density (ΔP). According to our previous work,[13] the polarization induced interface charges can be partially compensated by those ionized external dopants in the quantum barriers, and thus, the electric field in the quantum wells can be reduced. In this work, those ionized external dopants in Ref. 13 have been substituted by the polarization induced bulk charges.

According to Fig. 4, in which the In$_x$Ga$_{1-x}$N layer with the linearly graded InN composition is embedded in the two InGaN layers, we have $+\sigma_{S1}^{Pol}$ and $-\sigma_{S2}^{Pol}$ at the two interfaces while $-\rho_B^{Pol}$ in the In$_x$Ga$_{1-x}$N layer if x is linearly increased along the [0001] growth orientation within the In$_x$Ga$_{1-x}$N layer thickness of l_b. If there are no external dopants in the In$_x$Ga$_{1-x}$N layer, then the net polarization charge density (ΔP) is not a constant, and instead, it can be expressed by the following equation:

$$\Delta P(z) = \sigma_{S1}^{Pol}|_{z=0} - \rho_B^{Pol} \cdot z \quad (z < l_b). \tag{3}$$
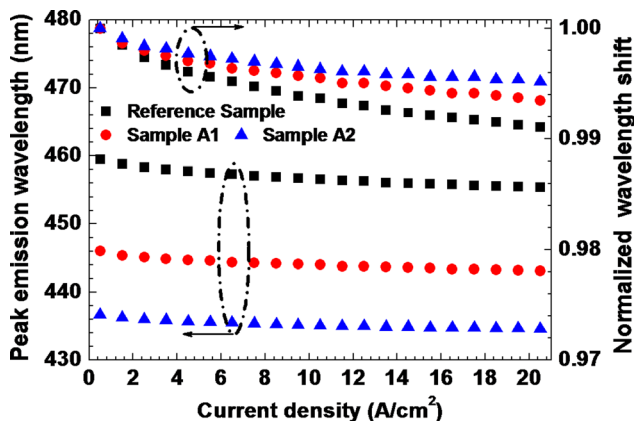

FIG. 3. Peak emission wavelengths in terms of the injection current levels, along with which also shows the normalized wavelength shifting levels with the increasing current density.
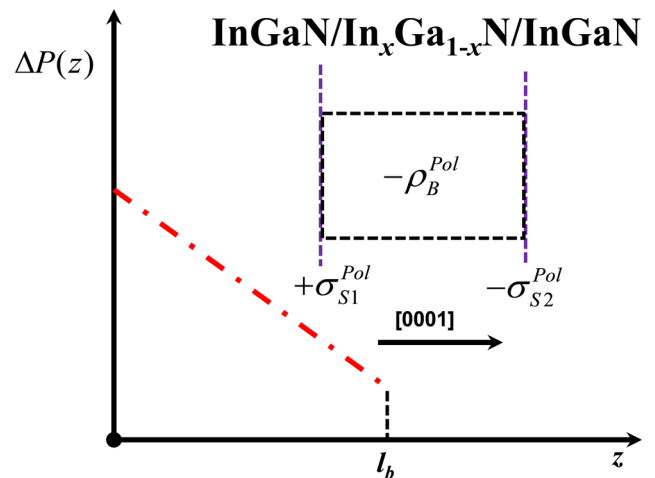

FIG. 4. Schematic diagram of the net polarization charge density in terms of the grading position. Inset figure shows the charge profile for the InGaN/In$_x$Ga$_{1-x}$N/InGaN heterostructure that has the graded InN composition in the In$_x$Ga$_{1-x}$N layer. The x is linearly increased along the [0001] orientation.

Thus, it shows that the net polarization charges can be screened by the polarization induced bulk charges. $\Delta P(z)$ can be further reduced by increasing ρ_B^{Pol}, which can be realized through increasing the grading level (e.g., Samples A1 and A2). Moreover, $\Delta P(z)$ also follows a linear relationship with the grading position (z) in the $In_xGa_{1-x}N$ layer and hence $E_b(z)$. Therefore, $\int_0^{l_b} E_b(z) \cdot dz = E_w \cdot l_w$ is still valid.

Besides the qualitative interpretation, we have also precisely demonstrated the electric field profiles for the reference sample, Samples A1 and A2 through numerical simulations by APSYS.[13] The polarization induced charges used in the simulation have been summarized in Table I. Other simulation parameters such as the Shockley-Read-Hall recombination lifetime of 43 ns, Auger recombination coefficient of 1×10^{-30} cm^6/s, and the band offset ratio of 70/30 for the InGaN/GaN MQW can also be found in our previously published works.[13,18–22]

The electric field profiles under the equilibrium have been shown in Fig. 5(a). As illustrated, the electric field profiles in the quantum barriers linearly vary with the growth orientation, which is consistent with Eqs. (2b) and (3). It can be clearly seen that the electric field magnitude both in the quantum barriers and the quantum wells of the MQW region for the Samples A1 and A2 is smaller than that for the reference sample. Moreover, Sample A2 has demonstrated an even better screening effect to the polarization induced electric field when compared to Sample A1 which is due to the

larger polarization induced bulk charge density in the quantum barriers as shown in Table I.

Besides the strong polarization induced electric field in the quantum wells for the [0001] oriented InGaN/GaN LEDs, another obstacle substantially hindering the quantum efficiency is the low hole injection efficiency. The hole injection efficiency is adversely affected when Si-doped quantum barriers are incorporated into the InGaN/GaN MQW stack with the aim to suppress the polarization induced electric field in the MQWs.[13] However, the hole blocking effect is mitigated in the proposed samples which will be shown here. We have demonstrated the simulated hole profiles at 20 A/cm^2 for the reference sample, Samples A1 and A2 in Fig. 5(b), respectively. The improved hole transport has been obtained from Samples A1 and A2 with holes in Sample A2 penetrating the deepest across the MQW region when compared to the reference sample. The improved hole transport in Samples A1 and A2 results from the reduced average effective valance band barrier height for holes when the $In_xGa_{1-x}N$ quantum barriers replace the GaN quantum barriers in the reference sample. Note that the even more asymmetric valance band profile between QB0 and QB1 for Sample A2 than for Sample A1 causes the strong hole accumulation in QW1 for Sample A2.

Therefore, the constructive combination of the reduced polarization induced electric field and the improved hole injection in the proposed structures is helpful in increasing the radiative recombination rates, and thus the optical performance of the LEDs as shown in Fig. 6. The optical output powers of Sample A1 and Sample A2 have been roughly improved by 46.15% and 42.31% compared to that of the reference sample at 100 A/cm^2, respectively. The external quantum efficiency (EQE) is also improved as demonstrated in Fig. 6, which directly illustrates the ratio between the emitted photon number and the injected electron number. Furthermore, according to Fig. 6, Sample A1 performs slightly better than Sample A2 in optical output power and EQE though Sample A2 has a smaller polarization induced electric field in the quantum wells and better hole injection than Sample A1. This is possibly due to the reduced electron confinement efficiency in Sample A2 when the average InN composition in the quantum barriers has been increased. Hence, to reduce the electron overflow while
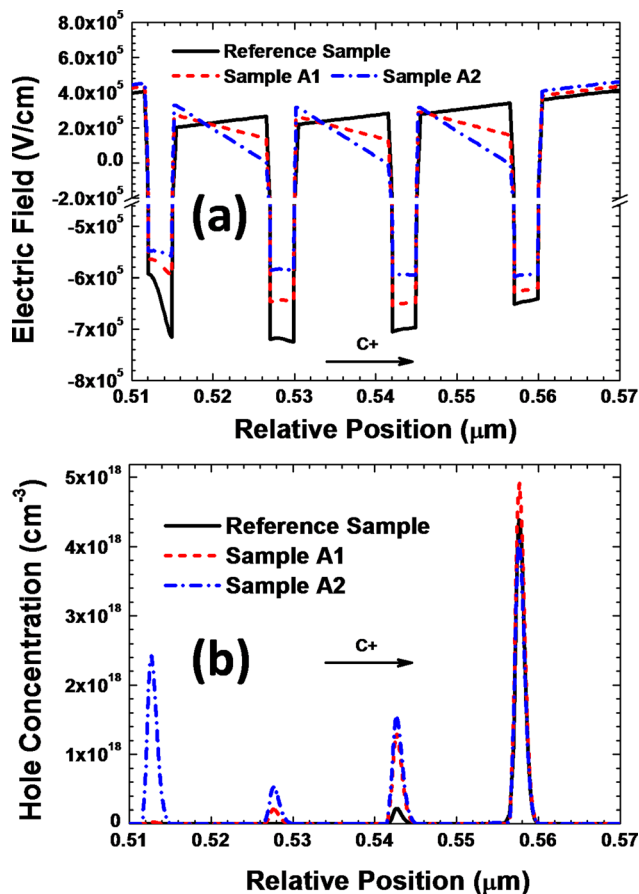

FIG. 5. (a) Electric field profile at the equilibrium. The positive direction of the electric field is along the C+ orientation, (b) simulated hole concentration at 20 A/cm^2.
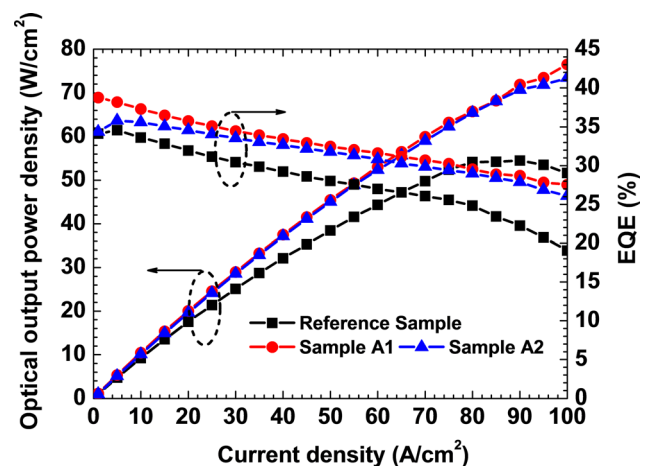

FIG. 6. Experimentally measured optical output power density and EQE as a function of the injection current levels.

keeping an improved hole injection, one can properly optimize the number of quantum barriers, of which the InN composition is graded.

To summarize, we have proposed and demonstrated the self-screening effect of the polarization induced bulk charges on the QCSE both experimentally and theoretically. With the alloy composition properly graded in the quantum barriers, on one hand, the QCSE in the quantum wells can be suppressed, and on the other hand, the hole transport can be enhanced. Our findings suggest that the proposed quantum barriers with InN composition grading along the growth orientation can be a very promising method for high-efficiency LED.

[1]S. T. Tan, X. W. Sun, H. V. Demir, and S. P. DenBaars, IEEE Photonics J. **4**, 613–619 (2012).

[2]J. Cho, E. F. Schubert, and J. K. Kim, Laser Photonics Rev. **7**, 408–421 (2013).

[3]Y. Li, S. You, M. Zhu, L. Zhao, W. Hou, T. Detchprohm, Y. Taniguchi, N. Tamura, S. Tanaka, and C. Wetzel, Appl. Phys. Lett. **98**, 151102 (2011).

[4]G. Verzellesi, D. Saguatti, M. Meneghini, F. Bertazzi, M. Goano, G. Meneghesso, and E. Zanoni, J. Appl. Phys. **114**, 071101 (2013).

[5]J. Hader, J. V. Moloney, and S. W. Koch, Appl. Phys. Lett. **96**, 221106 (2010).

[6]E. Kioupakis, P. Rinke, K. T. Delaney, and C. G. Van de Walle, Appl. Phys. Lett. **98**, 161107 (2011).

[7]E. Kioupakis, Q. Yan, and C. G. Van de Walle, Appl. Phys. Lett. **101**, 231107 (2012).

[8]S.-C. Ling, T.-C. Lu, S.-P. Chang, J.-R. Chen, H.-C. Kuo, and S.-C. Wang, Appl. Phys. Lett. **96**, 231101 (2010).

[9]X. Li, X. Ni, J. Lee, M. Wu, Ü. Özgür, H. Morkoç, T. Paskova, G. Mulholland, and K. R. Evans, Appl. Phys. Lett. **95**, 121107 (2009).

[10]A. E. Romanov, T. J. Baker, S. Nakamura, J. S. Speck, and E. J. U. Group, J. Appl. Phys. **100**, 023522 (2006).

[11]C. Roberts, Q. Yan, M.-S. Miao, and C. G. Van de Walle, J. Appl. Phys. **111**, 073113 (2012).

[12]J. Y. Chang and Y. K. Kuo, Opt. Lett. **37**, 1574–1576 (2012).

[13]Z.-H. Zhang, S. T. Tan, Z. Ju, W. Liu, Y. Ji, Z. Kyaw, Y. Dikme, X. W. Sun, and H. V. Demir, J. Disp. Technol. **9**, 226–233 (2013).

[14]Z.-H. Zhang, S. T. Tan, Z. Kyaw, W. Liu, Y. Ji, Z. Ju, X. Zhang, X. W. Sun, and H. V. Demir, Appl. Phys. Lett. **103**, 263501 (2013).

[15]V. Fiorentini, F. Bernardini, and O. Ambacher, Appl. Phys. Lett. **80**, 1204–1206 (2002).

[16]M. V. Durnev, A. V. Omelchenko, E. V. Yakovlev, I. Y. Evstratov, and S. Y. Karpov, Phys. Status Solidi A **208**, 2671–2675 (2011).

[17]J. Piprek, *Nitride Semiconductor Devices Principles and Simulation* (Wiley-VCH Verlag GmbH & Co. KGaA, Weinheim, 2007).

[18]Z.-H. Zhang, S. T. Tan, Y. Ji, W. Liu, Z. Ju, Z. Kyaw, X. W. Sun, and H. V. Demir, Opt. Express **21**, 15676–15685 (2013).

[19]Z.-H. Zhang, S. T. Tan, Z. Kyaw, Y. Ji, W. Liu, Z. Ju, N. Hasanov, X. W. Sun, and H. V. Demir, Appl. Phys. Lett. **102**, 193508 (2013).

[20]Y. Ji, Z.-H. Zhang, Z. Kyaw, S. T. Tan, Z. G. Ju, X. L. Zhang, W. Liu, X. W. Sun, and H. V. Demir, Appl. Phys. Lett. **103**, 053512 (2013).

[21]Z. G. Ju, W. Liu, Z.-H. Zhang, S. T. Tan, Y. Ji, Z. B. Kyaw, X. L. Zhang, S. P. Lu, Y. P. Zhang, B. B. Zhu, N. Hasanov, X. W. Sun, and H. V. Demir, Appl. Phys. Lett. **102**, 243504 (2013).

[22]Z.-H. Zhang, S. T. Tan, W. Liu, Z. Ju, K. Zheng, Z. Kyaw, Y. Ji, N. Hasanov, X. W. Sun, and H. V. Demir, Opt. Express **21**, 4958–4969 (2013).